

Synthesis and Self-Assembly of Fluorescent Micelles from Poly(ferrocenyldimethylsilane-*b*-2-vinylpyridine-*b*-2,5-di(2'-ethylhexyloxy)-1,4-phenylvinylene) Triblock Copolymer

Feng He,[†] Torben Gädt,[‡] Marcus Jones,[†] Gregory D. Scholes,[†] Ian Manners,^{*,‡} and Mitchell A. Winnik^{*,†}

[†]Department of Chemistry, University of Toronto, 80 St. George Street, Toronto, Ontario M5S 3H6, Canada, and [‡]School of Chemistry, University of Bristol, Bristol BS8 1TS, U.K.

Received May 11, 2009; Revised Manuscript Received August 13, 2009

ABSTRACT: A fluorescent ABC triblock copolymer containing poly(ferrocenyldimethylsilane) (PFS) and poly(2-vinylpyridine) (P2VP) moieties in the segments was synthesized via living anionic polymerization followed by quenching the living chains using a π -conjugated poly(2,5-di(2'-ethylhexyloxy)-1,4-phenylvinylene aldehyde (PDEHPV-CHO) homopolymer. The resulting triblock copolymer poly(ferrocenyldimethylsilane-*b*-2-vinylpyridine-*b*-2,5-di(2'-ethylhexyloxy)-1,4-phenylvinylene) (PFS-*b*-P2VP-*b*-PDEHPV) underwent self-assembly in 2-propanol to form cylindrical micelles. 2-Propanol is a good solvent for P2VP, a modest solvent for PDEHPV, and a poor solvent for PFS. The cylindrical shape of the micelles is likely related to the semicrystalline nature of the PFS in the core. The PDEHPV block showed strong green-yellow fluorescence both for polymers dissolved as discrete molecules in tetrahydrofuran (THF), a good solvent for all three components, and as micelles in 2-propanol. The fluorescence quantum yields were 56% for the triblock copolymer in THF and ca. 17% for the micelles in 2-propanol. Because ferrocene units are powerful fluorescence quenching entities, we surmise that in both cases, the P2VP block acts as a spacer to minimize the quenching of PDEHPV fluorescence by the PFS block. Taking advantage of the fluorescence of the PDEHPV block, we were able to obtain images of the block copolymer micelles and their flower-like aggregates in 2-propanol solution by laser confocal fluorescence microscopy.

Introduction

Metal-containing polymers are attracting growing interest as functional materials. Many interesting properties arise through incorporation of metal atoms in the polymeric architecture.^{1–6} Polymers containing ferrocene take advantage of its inherent organic and inorganic nature,⁷ which include its high thermal stability, good solubility in organic media, versatility in the synthesis of derivatives,⁸ and reversible redox reactivity^{9,10} associated with oxidation of the iron center.¹¹ We are particularly interested in amphiphilic block copolymers with ferrocene in the backbone of one of the blocks. One fascinating set of examples are the poly(ferrocenyldimethylsilane) (PFS)-based diblock copolymers.¹² In the bulk state, these polymers behave normally and self-assemble to form periodic structures. Depending on the relative lengths of the two blocks, one can find spheres,¹³ hexagonally packed cylinders, and lamella.^{14,15} Thin films of these periodic structures have been utilized as resists for patterning silicon wafers.¹⁶

PFS diblock copolymers form micelles in a variety of selective solvents. In poor solvents for PFS that are good solvents for the other block, micelles form with a dense PFS core surrounded by a solvent swollen corona of the other block. What is unusual about these polymers is that they form cylindrical micelles for a wide range of compositions in which the PFS is the shorter block.¹⁷ This behavior is strikingly different than that of most diblock copolymers in selective solvents, which form cylindrical micelles only for a narrow range of compositions in which the insoluble block is the longer block.¹⁸ This unusual morphology has been attributed to the semicrystalline nature of the PFS core in the

micelles.¹⁹ While the effect of a crystalline micelle core has not yet been shown to be general, there are now several examples of block copolymers with a corona block much longer than its crystalline core block that form fiber-like micelles in selective solvents. These examples for the crystalline block include polyacrylonitrile,^{20,21} poly(ferrocenylgermane),¹⁹ poly(ϵ -caprolactone),²² the complex formed by poly-D-lactide and poly-L-lactide,²³ and an ABC triblock copolymer with a polyethylene middle block.²⁴ Early examples in the literature of micelle formation by diblock copolymers in which the core-forming block was crystalline (poly(ethylene oxide) in hydrocarbon solvents,²⁵ polyethylene²⁶) described planar structures for the micelles. We have also found raft-like planar structures for PFS diblock copolymers in which the corona-forming block was shorter than the PFS block.²⁷ If the ferrocene block is unable to crystallize, or if the PFS core remains amorphous, the polymers form conventional spherical micelles.^{28,29}

Another unique feature of cylindrical PFS block copolymer micelles is that they increase in length by a nucleated growth mechanism that has many of the characteristics of a living polymerization.^{19,30} Preformed short micelles in solution act as seeds. When additional block copolymer is added to the solution, it condenses onto the ends of existing micelles. In this way, rod-like micelles with a relatively narrow distribution of lengths can be obtained. We have recently drawn an analogy between the growth mechanism of rod-like PFS block copolymer micelles in selective solvents and the growth of amyloid fibers in aqueous media.³¹

Other research groups have been interested in the idea of introducing ferrocene units into conjugated polymers. One of the ideas behind this research is to be able to couple the redox activity of the ferrocene unit with the conducting, semiconducting, or photoluminescent properties of the conjugated polymers. In addition, there was the hope that the excellent self-assembly properties

*Corresponding authors. E-mail: (M.A.W.) mwinnik@chem.utoronto.ca; (I.M.) ian.manners@bristol.ac.uk.

of ferrocene-containing copolymers would enhance thin film device applications, in which the film morphology would have a positive influence on the final device performance. Polymers of this type have been prepared by condensation polymerization with difunctional ferrocenyl monomers^{32–34} or by more controlled methods such as ring-opening metathesis polymerization of ferrocenophanes.^{35–37} These materials have shown potential applications in optoelectronics, via enhanced conductivity upon doping,³³ second-order nonlinear optical properties³⁸ and via their photovoltaic response.³⁹ Very few publications report high fluorescence quantum yields for conjugated polymer-based copolymers with ferrocene because the ferrocene-unit can quench the fluorescence of the chromophores.^{40–42} There are two possible mechanisms for this quenching. The most likely involves “charge transfer” in which the ferrocene acts as an electron donor.^{43,44} Also possible is energy transfer via the Förster^{32,33} or Dexter⁴⁵ mechanisms, followed by rapid nonradiative decay of the excited ferrocene. Both quenching mechanisms require close proximity between the conjugated chromophores and the quenching group.⁴⁵

Here we report the synthesis and self-assembly properties of an ABC triblock copolymer, in which the A-block is PFS, and the C-block is poly(2,5-di(2'-ethylhexyloxy)-1,4-phenylvinylene), which we refer to as PDEHPV. PDEHPV is a highly fluorescent polymer that exhibits good solubility in a variety of solvents of intermediate polarity, such as toluene, THF, chloroform, and dichloromethane, and limited solubility in alcohols. Separating the PFS and PDEHPV blocks is a relatively long poly(2-vinylpyridine) (P2VP) B-block. In alcohol solvents, such as 2-propanol, this triblock copolymer forms cylindrical micelles with a PFS core and a P2VP corona, as has been shown previously for PFS-*b*-P2VP diblock copolymers.⁴⁶ The questions of interest are how micellization is affected by the terminal PDEHPV block and how incorporation of the conjugated polymer into the structure and into the micelles affects their fluorescent properties.

Experimental Section

Materials and Instrumentation. Methylhydroquinone (99%, Aldrich), 2-ethylhexyl bromide (95%, Aldrich), phosphoryl chloride (99%, Aldrich), aniline (99%, Aldrich), potassium *tert*-butoxide (97%, Aldrich), *n*-butyllithium (1.6 M in hexanes, Acros), trioctylaluminum (25 wt % in hexanes, Aldrich) were used as received. 2-Vinylpyridine (97%, Aldrich) was purified by distillation first over CaH₂. A second distillation from trioctylaluminum was performed immediately before the polymerization. 1,1-Diphenylethylene (DPE) (97%, Aldrich) was titrated with *n*-butyllithium until a deep red color sustained and then distilled under high vacuum. 1,1-Dimethylsilacyclobutane (DMSB) (97%, Aldrich) was distilled over CaH₂ twice. Lithium chloride (99.99%, Aldrich) was vacuum-dried at 120 °C overnight. THF was distilled under reduced pressure from Na/benzophenone before polymerization. [1]Dimethylsilaferrocenophane was synthesized according to a methodology reported previously in the literature.⁴⁷

¹H NMR spectra were recorded on a Varian 400 spectrometer with deuterated benzene as solvent. Molecular weights were determined by a Viscotek GPC MAX liquid chromatograph equipped with a triple detector array (Model 302, Viscotek) and a UV detector (Model 2501, Viscotek). Polystyrene standards (Aldrich) were used for calibration, and a solution of 2% triethylamine in THF was used as the eluent. UV–vis absorption spectra were collected on a Perkin-Elmer Lambda 25 spectrometer using 1.00 cm quartz cuvettes.

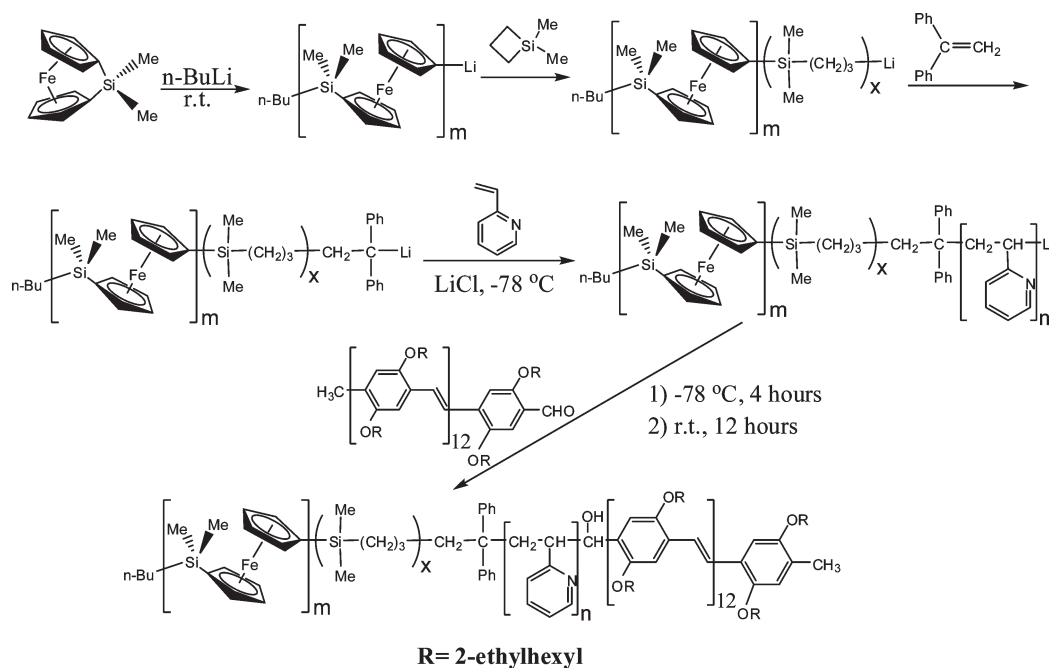
Synthesis and Characterization of PDEHPV-CHO (1). Poly(2-ethylhexyloxy)phenylvinylene aldehyde (PDEHPV-CHO) (1) was synthesized by Siegrist polycondensation,^{48,49} following a

procedure reported by Olsen and Segalman.³⁶ At the last step of the polymerization, 3 equiv of potassium *tert*-butoxide (21 mmol, 2.36 g) was added to 300 mL of dry DMF and heated to 40 °C. 2,5-Di(2'-ethylhexyloxy)-4-methyl-*N*-benzylideneaniline was added dropwise and allowed to react for another 30 min. The reaction mixture was poured into acidified water and stirred for 48 h to hydrolyze the unreacted imines. The product was collected, neutralized, and purified by silica gel column chromatography. The value of $M_n = 4700$ g/mol and the number-average degree of polymerization $n = 13$ for PDEHPV-CHO was determined by ¹H NMR in CDCl₃ using the aldehyde peak at 10.4 ppm as reference (Figure S4, Supporting Information). The polydispersity index was measured at 1.20 by gel permeation chromatography (GPC) in THF using polystyrene standards. PDEHPV-CHO was dried on a Schlenk line overnight before using it for the preparation of the triblock copolymer.

The limiting solubility of this PDEHPV-CHO sample in 2-propanol was estimated by UV–vis absorption spectroscopy in conjunction with a Beer–Lambert law analysis assuming that the extinction coefficient for the polymer in THF, a good solvent for the polymer, is similar to that for the polymer in 2-propanol. Four different concentrations ($c = 0.050, 0.010, 0.0050$, and 0.0010 mg/mL) of polymer were prepared by weighing out individual samples on a microbalance and dissolving them into known weights of THF. Measurements of absorbance at $\lambda_{\max} = 483$ nm vs weight concentration (Figure S2, Supporting Information) was linear and passed through the origin. From the slope of the line, we calculated an extinction coefficient of $\epsilon_{483} = 43.7$ mL mg^{−1} cm^{−1}. Then a 2-propanol solution containing excess PDEHPV₁₃-CHO (ca. 0.1 mg/mL) was heated at 80 °C for 1 h and cooled to room temperature. After filtering this yellow solution through a 0.2 μ m filter to remove undissolved polymer, the UV–vis spectrum of this solution was measured. From $A = 0.87$ and assuming that the extinction coefficient for the compound in THF is the same as that in 2-propanol, we calculated a saturation weight concentration of ca. 0.02 mg/mL for PPV homopolymer in 2-propanol.

Synthesis of PFS-*b*-P2VP-*b*-PDEHPV Triblock Copolymer (4). PFS-*b*-P2VP was prepared by anionic polymerization following the procedure reported by Wang et al.⁴⁶ In a N₂-filled glovebox at room temperature, 29.8 μ L of *n*-BuLi (1.6 M in hexanes) was added quickly to a stirred solution of [1]dimethylsilaferrocenophane (300 mg, 1.24 mmol) in THF (2 mL). After 1 h, the color of the solution changed from red to amber indicating complete conversion of the monomer. To determine the molecular weight and PDI of the PFS block, an aliquot (0.2 mL) of the living PFS homopolymer solution was quenched with degassed methanol. Then DPE (33.6 μ L, 0.19 mmol) was then added to the reaction, followed by DMSB (11.5 μ L, 0.086 mmol). After the color changed from amber to deep red within a few minutes, the reaction vial was removed to the cold well (−78 °C) in the glovebox cooled with a dry ice-acetone bath. A second vial with a solution of dried LiCl (14.6 mg, 0.34 mmol) and 2-vinylpyridine (1.02 mL, 9.46 mmol) in THF (5.6 mL) was also cooled to −78 °C before the two solutions were combined. The polymerization was left running at −78 °C for 1 h. An aliquot consisting of half of the reaction mixture was removed to obtain a sample of the PFS-*b*-P2VP diblock copolymer (3).

Then a small excess (1.1 molar equiv, 98.6 mg in 1 mL of distilled dry benzene) of PDEHPV-CHO homopolymer (1) was added to the reaction mixture, which was kept at −78 °C for 4 h and then allowed to warm to room temperature and stirred for an additional 12 h in the glovebox. (Prior to introduction in the reaction, the PDEHPV-CHO

Chart 1. Synthesis of PFS-*b*-P2 VP-*b*-PDEHPV Triblock Copolymer

homopolymer (**1**) was dried first by azeotropic distillation: it was dissolved in distilled toluene and evaporated at 50 °C under reduced pressure three times. Then it was dried overnight at 50 °C on a Schlenk line before being transferred into the glovebox.) Then the reaction mixture was removed from the glovebox, and a few drops of degassed methanol were added into the solution. After precipitation of the solution into hexanes, the orange solid obtained was dissolved in 2 mL of THF and then added to hexanes drop by drop to precipitate the triblock copolymer. This procedure was repeated three times, and then followed by drying overnight under vacuum to give 760 mg of triblock polymer (yield: 45%). The polymer obtained was further purified by repeated size exclusion column chromatograph (HW-55F from TOSOH, Japan) using 2% triethylamine in THF as the eluent until no PFS and PDEHPV-CHO homopolymer could be detected by a UV detector (450 nm) on the GPC.

¹H NMR δ (ppm, C₆D₆): 0.56 (s, Si(CH₃)₂), 0.78–1.45 (m, CH₃, CH₂ and CH, PDEHPV), 1.90–2.95 (m, CH₂ and CH, P2VP), 3.87–4.03 (m, OCH₂), 4.12 (m, Cp), 4.28 (m, Cp), 6.33–7.10 (m, aromatic protons, P2VP), 7.62 (CH=, PDEHPV), 8.15 (aromatic protons, PDEHPV) 8.40 (m, NCHC). GPC: M_n (PDI): 7300 (1.06) for the PFS block (triple detector system, Figure S1, Supporting Information), 30400 (1.17) for the PFS-*b*-P2VP diblock copolymer and 32500 (1.20) for PFS-*b*-P2VP-*b*-PDEHPV triblock copolymer.

¹H NMR spectra of the PDEHPV-CHO homopolymer (**1**), PFS-*b*-P2VP diblock copolymer (**3**), and the PFS-*b*-P2VP-*b*-PDEHPV triblock copolymer (**4**) are presented in the Supporting Information.

Preparation of Block Copolymer Micelles. Solid samples of the triblock copolymer (ca. 1 mg) were added to vials (20 mL) containing 5 mL of 2-propanol to achieve a final concentration of typically 0.2 mg/mL. These solutions were heated at 80 °C for 1 h and then allowed to cool to room temperature in the open air. These solutions were used as is, or diluted for microscopy measurements. Some samples were sonicated hot, by placing a sealed vial (20 mL) containing 5 mL sample (0.05 mg/mL) taken from the 80 °C oil bath and immersing it immediately into the water bath of the ultrasonic cleaning bath at ca. 23 to 25 °C for 10 min.

Fluorescence and Microscopy Measurements. Fluorescence (FL) spectra were measured using a SPEX Fluorolog-3 spectrofluorometer (Jobin Yvon/SPEX, Edison, NJ). Fluorescence decay profiles were measured by time-correlated single photon counting,⁵⁰ using picosecond excitation pulses from a Spectra-Physics MillenniaXs-P Ti-sapphire laser, pumped with a solid-state diode laser emitting at 532 nm. A picosecond pulse selector and a frequency doubler were used in order to adjust the repetition rate of the laser to ca. 8 MHz and the wavelength to 480 nm. The short-time resolution of the instrument is ca. 30 ps (ca. 14% fwhm of the instrument response). The data were analyzed using a least-squares fitting algorithm involving the iterative deconvolution of a model exponential decay function with the measured instrument response function.

TEM images were obtained using a Hitachi H-7000 transmission electron microscope operating at 100 kV. Samples for TEM experiments were prepared by drying a drop of solution on a Formvar and carbon-coated copper grid. The micelle solution was diluted to about 0.05 mg/mL and most of the solution on the grid was absorbed by touching the edge of the drop with a filter paper. The laser confocal fluorescence microscopy (LCFM) images were obtained using a laser scanning confocal microscope (Leica TCS SP2) with a 63 \times oil objective, NA = 1.4 at λ_{ex} = 488 \pm 20 nm and λ_{em} = 560 \pm 25 nm. The samples for LCFM were prepared by sealing one drop of a micelle solution in 2-propanol (~0.001 mg/mL) between a microscopy slide and a coverslip to prevent solvent evaporation. Wide-angle X-ray scattering (WAXS) data were obtained using a Siemens D500 diffractometer equipped with a Cu K α X-ray source. The samples for WAXS experiments were prepared by casting a solution of micelles 3 days after it was prepared onto a silicon wafer and allowing the solvent to evaporate at ambient temperature.

Results and Discussion

Synthesis and Characterization of PFS-*b*-P2VP-*b*-PDEHPV Triblock Copolymer. The design of our approach to the preparation of the PFS-*b*-P2VP-*b*-PDEHPV triblock copolymer, as shown in Chart 1, was based upon our previous report⁴⁶ of the synthesis of PFS-*b*-P2VP block copolymers. A key feature

of this synthesis is the conversion of the living PFS carbanion to a more reactive diphenylmethyl carbanion via a strategy developed by Rehahn et al.^{51,52} in which a mixture of 1,1-dimethylsilacyclobutane (DMSB) and 1,1-diphenylethylene (DPE) in a 2/4 ratio relative to the PFS homopolymer living chains was added to the reaction after the polymerization of the [1]dimethylsilaferrocenophane monomers. After subsequent polymerization of 2-vinylpyridine at $-78\text{ }^{\circ}\text{C}$, the living end group was quenched with the poly(phenylvinylene) aldehyde derivative as shown in Chart 1. This PDEHPV-CHO homopolymer was prepared independently by Siegrist polycondensation^{48,49} and added in slight (10% mol) excess as a solution in benzene to the reaction mixture at $-78\text{ }^{\circ}\text{C}$.

The quenching efficiency was determined both by NMR and FT-IR, as the aldehyde peak of the homopolymer appeared at 10.4 ppm in NMR and 1680 cm^{-1} in FT-IR. These peaks disappeared completely in the purified triblock copolymers (Figure S3, Supporting Information), which suggested that the triblock copolymer was free of PDEHPV-CHO homopolymer. During the reaction, aliquots of the PFS homopolymer and PFS-*b*-P2VP diblock copolymer were taken at the appropriate times for GPC analysis.

For the PFS homopolymer, the absolute value of the molecular weight was determined by triple detection GPC analysis using THF as the eluent. M_n for the PDEHPV-CHO homopolymer was determined by end group analysis by ^1H NMR using the one-proton signal of the aldehyde at 10.4 ppm as a reference. The molecular weights and molecular weight distributions of the block copolymers were estimated by GPC using a mixture of 2% triethylamine in THF as the eluent. Figure 1A shows representative GPC traces of a PFS-*b*-P2VP-*b*-PDEHPV triblock copolymer and its precursor PFS-*b*-P2VP diblock copolymer as well as the first block, PFS. The polydispersity of the triblock copolymer is 1.2. Because the molecular weight of the PPV block is about 4700 g/mol, the GPC trace of the triblock copolymer shows only a small shift compared with that of the diblock copolymer. Nevertheless, it is clear that the peak maximum of the triblock copolymer moves to lower retention volume without any shoulder peaks, which indicates that the PDEHPV-CHO reacted efficiently with the diblock living chain to achieve the desired triblock copolymer. In addition, the UV-vis trace of the triblock copolymer, monitored at

450 nm and presented in Figure 1B, exhibits a single symmetric peak. The signal at this wavelength is combination of the absorbances of the PFS and PDEHPV blocks. The characteristics of the block copolymer and its components are summarized in Table 1.

The composition of the triblock copolymer (i.e., the block ratios) was determined by ^1H NMR. In this analysis, the respective sizes of three blocks were determined by integrating peaks corresponding to the P2VP hydrogens at 6.6 ppm (2H, pyridine 2,6-positions), the PFS hydrogens at 4.3 ppm (4H per ferrocene unit), and the PDEHPV hydrogens at 4.0 ppm (2H, $-\text{OCH}_2-$). Representative spectra ^1H NMR spectra are presented in the Supporting Information (Figure S6). The calculated block ratio of PFS: P2VP: PDEHPV for this sample was 30: 300: 13. On the basis of ^1H NMR integration and the known densities of the respective homopolymers (PFS,¹⁴ 1.26; P2VP,⁵³ 1.15; and PDEHPV,⁵⁴ 0.988 g/cm³, respectively), we estimate that the volume fractions (ϕ) of the three blocks in the triblock copolymer are 0.15 (ϕ_{PFS}), 0.73 (ϕ_{P2VP}), and 0.12 (ϕ_{PDEHPV}).

Self-Assembly of PFS-*b*-P2VP-*b*-PDEHPV Triblock Copolymers in 2-Propanol. To obtain solutions of PFS₃₀-*b*-P2VP₃₀₀-*b*-PDEHPV₁₃ triblock copolymer in 2-propanol, it is necessary to heat mixtures of the solvent and polymer. For example, when a mixture containing 0.2 mg/mL was heated at $80\text{ }^{\circ}\text{C}$ for 1 h and then cooled to room temperature, a slightly turbid solution was obtained. As seen in Figure 2A, flower-like structures had formed. These structures appear to be clusters of fiber-like micelles. Individual fibers in these clusters have lengths on the order of $10\text{ }\mu\text{m}$ or more. The stiff fibrous nature of these fibers outside the central core of the cluster can be seen in the higher magnification image in Figure 2B.

The flower-like structures seen in Figure 2A resemble structures formed in hexane by a different triblock copolymer, PFS-*b*-PDMS-*b*-PFS, in which the long middle block of poly(dimethylsiloxane) is the soluble block, with shorter insoluble PFS blocks at both ends.⁵⁵ Careful inspection of the micrographs published in ref 55 show that while the overall size and shape of the structures are similar, the individual fiber-like structures emanating from the central core of the PFS-*b*-PDMS-*b*-PFS aggregates appear to be more flexible and less well-defined than those seen here in Figure 2B.

This type of self-assembly is different than that observed for PFS₃₀-*b*-P2VP₃₀₀ diblock copolymer. In 2-propanol, the diblock copolymer forms discrete stiff cylindrical micelles, with lengths less than $5\text{ }\mu\text{m}$ as can be seen in Figure S7 (Supporting Information). The core width, as determined from TEM images, is approximately 10 nm both for the PFS₃₀-*b*-P2VP₃₀₀ diblock copolymers micelles seen in Figure S7 and for the fiber-like structures of the triblock copolymer micelles seen in Figure 1B.

To test for crystallinity in the micelles, films of the micelle clusters (as seen in Figure 2) were deposited on a silicon wafer and examined by wide-angle X-ray scattering (WAXS) measurements. The results, shown in Figure 3, reveal that both micelle samples, the PFS₃₀-*b*-P2VP₃₀₀-*b*-PDEHPV₁₃ triblock copolymer micelles depicted in Figure 2, and the

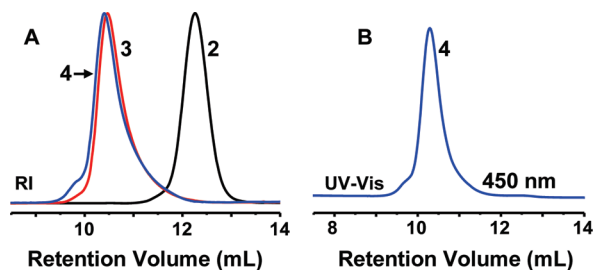


Figure 1. (A) GPC curves (refractive index) of PFS-*b*-P2VP-*b*-PDEHPV triblock copolymer (4) PFS-*b*-P2VP diblock copolymer (3) and their precursor PFS homopolymer (2). (B) UV-vis trace monitored at 450 nm of the triblock copolymer (4).

Table 1. Characterization of the PFS₃₀-*b*-P2VP₃₀₀-*b*-PDEHPV₁₃ triblock copolymer

polymer	M_n (PFS) ^a (g/mol)	M_n (diblock) ^b (g/mol)	molar ratio for diblock ^c	M_n (triblock) ^b (g/mol)	PDI ^d
PFS ₃₀ - <i>b</i> -P2VP ₃₀₀ - <i>b</i> -PDEHPV ₁₃ ^b	7300	30 400	1:10	32 500	1.20

^a Determined by triple detection GPC analysis using THF as the eluent. ^b Determined by conventional GPC analysis against polystyrene standards using (THF + 2% Et₃N) as the eluent. ^c Determined by ^1H NMR integration. ^d Determined from M_n of PFS homopolymer from triple detection GPC analysis and block ratios from ^1H NMR analysis as well as the ^1H NMR analysis of PDEHPV-CHO homopolymer.

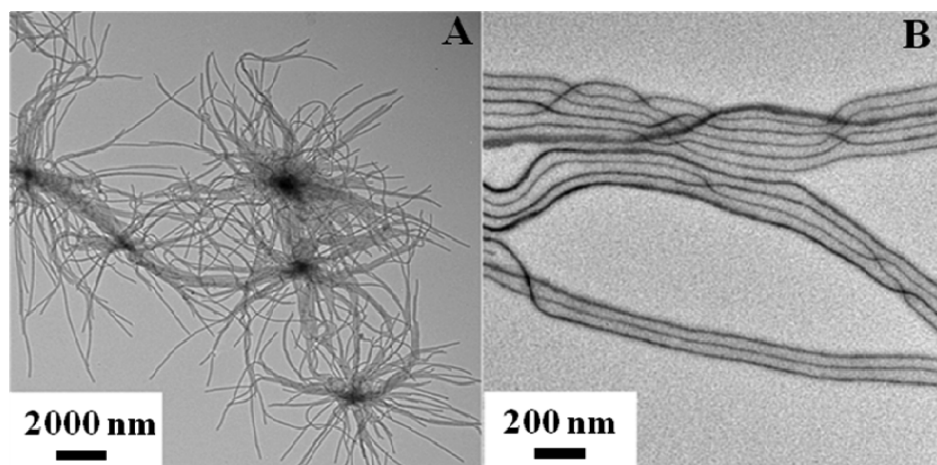


Figure 2. TEM images of $\text{PFS}_{30}\text{-}b\text{-P2VP}_{300}\text{-}b\text{-PDEHPV}_{13}$ micelles prepared in 2-propanol at 80 °C and 0.2 mg/mL followed by cooling to room temperature. The solution was diluted to 0.004 mg/mL before the preparation of the TEM grid. The image in B is a section of A at higher magnification.

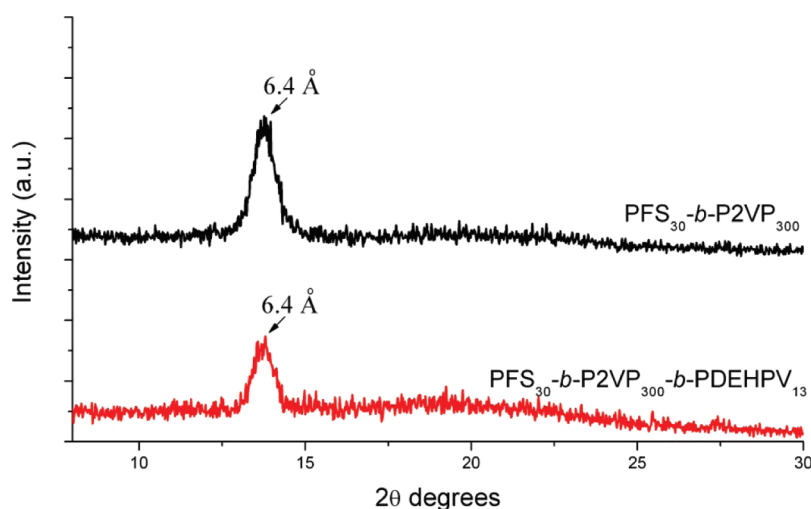


Figure 3. WAXS patterns for $\text{PFS}_{30}\text{-}b\text{-P2VP}_{300}\text{-}b\text{-PDEHPV}_{13}$ and $\text{PFS}_{30}\text{-}b\text{-P2VP}_{300}$ micelles prepared from 2-propanol. The sample was prepared by casting each solution of micelles onto a silicon wafer and allowing the solvent to evaporate at room temperature.

$\text{PFS}_{30}\text{-}b\text{-P2VP}_{300}$ diblock copolymers micelles seen in Figure S7 show the same peak corresponding to a d -spacing of 6.4 Å, which can be assigned to the distance between adjacent planes of the ferrocenylsilane groups within the PFS core of the micelles. The basic structure of the PFS core appears not to be influenced by the presence of the PDEHPV block at the end of each polymer molecule.

When a solution of these micelle aggregates was subjected to relatively mild sonication (immersion of a vial containing micelles into a 70 W cleaning bath for 10 min), the aggregates fragmented to yield much shorter rod-like micelles with little indication of aggregation. An example is shown in Figure 4. In this sample, which was still warm when immersed into the water of the cleaning bath (at ca. 23 °C), the micelles range in length from 40 to 300 nm. If the solution of micelle clusters was aged at room temperature before sonication, we also found rod-like micelles with no indication of aggregation, but a broader range of micelle lengths. The importance of these experiments is that they show that micelle aggregation as seen in Figure 2 is a property of long micelles. No significant aggregation could be seen in TEM images of micelles shortened by sonication.

The flower-like aggregates seen in solution for longer micelles is almost certainly a consequence of the PDEHPV

block of the triblock copolymer, since there is strong evidence against aggregation for cylindrical micelles of any length for $\text{PFS-}b\text{-P2VP}$ in 2-propanol.⁵⁶ If the PDEHPV block were insoluble in 2-propanol, one might imagine that there would be a strong driving force for this block to aggregate or to bury itself against the PFS core of individual micelles. To help us understand the contribution of PDEHPV solubility in 2-propanol to the behavior of the micelles, we carried out experiments to measure this solubility. As described in the Experimental Section, we prepared solutions of PDEHPV-CHO in THF, and constructed a Beer–Lambert plot to obtain an extinction coefficient of $\epsilon_{483} = 43.7 \text{ mL mg}^{-1} \text{ cm}^{-1}$. Assuming a similar value for the homopolymer in 2-propanol, we determined a limiting solubility of 0.02 g/mL. This value is well above the sample concentration of the triblock copolymer used to prepare the grids examined by TEM in Figure 2. But the local concentration of PDEHPV chains in the region of the micelle corona is likely to be above this limiting value, making aggregation of these chains possible.

Photophysical Properties of $\text{PFS-}b\text{-P2VP-}b\text{-PDEHPV}$ Triblock Copolymer and its Aggregates. The $\text{PFS-}b\text{-P2VP-}b\text{-PDEHPV}$ triblock copolymer forms homogeneous solutions in THF, a good solvent for all three of its components,

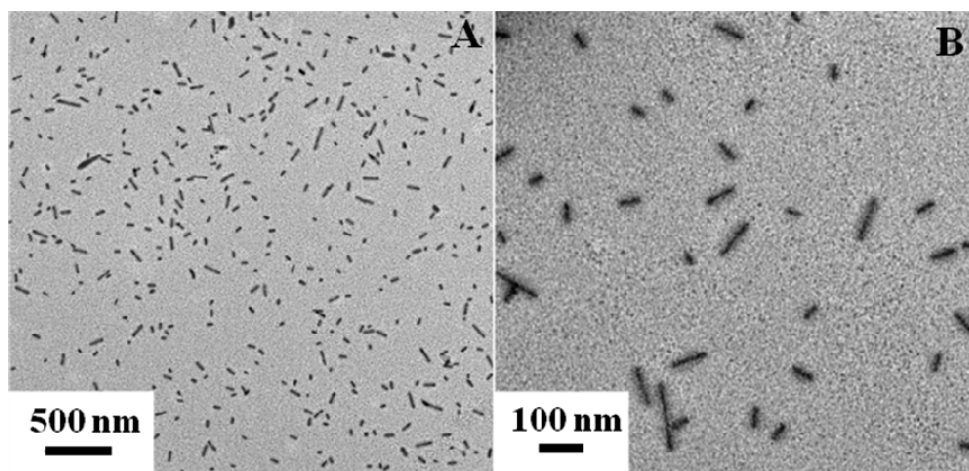


Figure 4. TEM images of PFS₃₀-*b*-P2VP₃₀₀-*b*-PDEHPV₁₃ micelles prepared by heating at 80 °C for 1 h in 2-propanol and then immersed while still warm into an ultrasonic cleaning bath. The bath temperature was 23 to 25 °C, and sonication was continued for 10 min. The TEM grid was prepared after the solution was aged 2 h at room temperature. The image in B is a section of A at higher magnification.

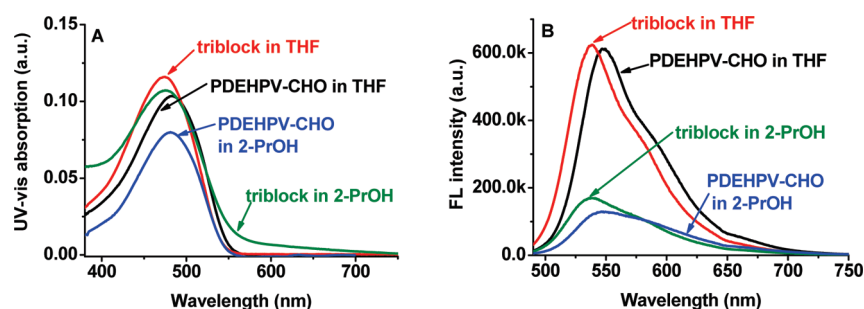


Figure 5. UV-vis (A) and fluorescence (B) spectra of the PFS₃₀-*b*-P2VP₃₀₀-*b*-PDEHPV₁₃ triblock copolymer and PDEHPV-CHO homopolymer in THF and in 2-propanol.

Table 2. Summary of Photophysical Properties of the Triblock Copolymer and PPV Homopolymer

polymers	solvent	$\lambda_{\text{max,abs}}$ (nm) ^a	$\lambda_{\text{max,em}}$ (nm) ^a	Φ_F ^b (%)	$\Phi_F/\Phi_F^{\text{THF}}$ ^c	τ^d (ps)	$\langle\tau\rangle/\langle\tau^{\text{THF}}\rangle^e$
PDEHPV-CHO	THF	483	548	61	1.0	527	1.0
PDEHPV-CHO	2-PrOH	481	547	18	0.30	222	0.42
triblock copolymer	THF	474	538	56	0.92	433	0.82
triblock copolymer	2-PrOH	475	539	17 ^e	0.28	322	0.61

^a In dilute solution (for triblock copolymer, 0.050 mg/mL both in THF and 2-PrOH; for PDEHPV-CHO homopolymer 0.0023 mg/mL in THF and 0.0019 mg/mL in 2-PrOH, calculated from the absorbance value at λ_{max} and $\epsilon_{483} = 43.7 \text{ mL mg}^{-1} \text{ cm}^{-1}$). ^b Using rhodamine 6G in absolute ethanol as the standard, $\lambda_{\text{ex}} = 480 \text{ nm}$. ^c Here Φ_F and the mean decay time $\langle\tau\rangle$ refer to the values of the PDEHPV-CHO homopolymer in THF solution. ^d Using picosecond excitation pulses, excited at 480 nm. ^e Apparent quantum yield in which the absorbance is not corrected for light scattering.

and, as we have described above, micelle-like aggregates form in 2-propanol. Here we focus on the spectroscopic properties, comparing the absorption and emission properties of the triblock copolymer with those of the PDEHPV-CHO. The UV-vis absorption spectra above 380 nm for the two polymers in THF and in 2-PrOH are shown in Figure 5A. The most important observation is that the λ_{max} for the PDEHPV-CHO is very similar in the two solvents and appears at slightly longer wavelength than λ_{max} for the triblock copolymers. The actual values are collected in Table 2. The small blue shift that accompanies formation of the triblock copolymer is likely due to the loss of the aldehyde group, which contributes additional conjugation in the homopolymer. Both triblock copolymer solutions are present at a concentration of 0.050 mg/mL. The solution in THF is characterized by $\lambda_{\text{max,abs}} = 474 \text{ nm}$. The solution in 2-PrOH was prepared by heating the solid material in 2-propanol (0.050 mg/mL) at 80 °C for 1 h and then allowing the solution to cool to room temperature. This micelle solution shows a maximal absorbance at 475 nm with

a long tail from 550 to 700 nm, which is consistent with a light scattering contribution to the spectrum.

Under UV excitation (365 nm), the triblock copolymer in THF solution shows a very strong green-yellow emission while the PDHPV-CHO homopolymer, by eye, shows a more yellow emission. As shown in Figure 5B, the wavelengths of the maximal emission ($\lambda_{\text{max,em}}$) in THF are 538 nm for the triblock copolymer and 548 nm for its PDHPV-CHO precursor. The corresponding peaks of those two polymers in 2-propanol are 539 (triblock copolymer) and 547 (PDEHPV-CHO homopolymer) nm, which are similar to their respective values in THF. In THF, the fluorescence quantum yield of the triblock copolymer is $\Phi_F = 0.56$, which is only slightly less than that of PDHPV-CHO in THF (0.61). The experimentally determined fluorescence quantum yield of the triblock copolymer micelles in 2-PrOH is about 1/3 ($\Phi_F = 0.17$) of that in THF, and close to that of PDEHPV-CHO homopolymer in 2-propanol ($\Phi_F = 0.18$). While this value is still significant and indicates that the micelles themselves exhibit substantial fluorescence, this value may in fact

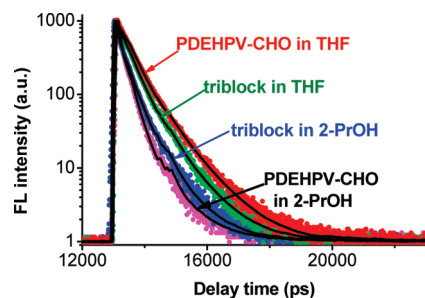


Figure 6. Normalized time-resolved fluorescent decay profiles of the triblock copolymer and PDEHPV-CHO homopolymer in solution.

underestimate the fluorescence efficiency of the PDHPV block within the micelles. From a technical perspective, the light scattering that contributes to the absorption spectrum as seen in Figure 5A makes it difficult to match the absorption of the micelle solutions to that of the Rhodamine 6G standard solution or to properly correct for absorbance differences. Thus, we take this as a minimum value.

For deeper insights into the luminescence properties of the species, we measured their fluorescence decay profiles following picosecond excitation. The decay profiles are presented in Figure 6. None of the traces exhibit linear decays when plotted semilogarithmically. These nonexponential decays are suggestive of a distribution of effective chromophores, each with its own characteristic lifetime. Each decay curve was fitted to a sum of three exponential terms, and intensity-weighted mean decay times were calculated from the normalized decays as $\langle\tau\rangle = \sum a_i \tau_i$. For PDEHPV-CHO the mean decay times are $\langle\tau\rangle = 527$ ps in THF, which drops to 222 ps for this molecule in 2-PrOH. As one can see in Table 2, the fractional decrease in mean decay time is similar in magnitude to the decrease in quantum yield associated with the change in solvent. The triblock copolymer has a mean decay time of 433 ps in THF and 322 ps in 2-propanol. One can see that the change in lifetime for the triblock copolymer is significantly smaller than for the PDEHPV-CHO homopolymer, and it is also smaller than the apparent change in fluorescence quantum yield. This result suggests that the light scattering superimposed on the absorption spectrum of the PDEHPV block of the micelles leads to an underestimation of its actual fluorescence quantum yield.

The most striking feature of these data is the high fluorescence quantum yield for the triblock copolymer, both in THF and in 2-PrOH. Given the strong tendency of ferrocene groups in general and PFS in particular to act as fluorescence quenchers,⁵⁷ these results indicate that there is little interaction between the PFS and PDEHPV blocks of the copolymer. In THF, which is a common good solvent for all three blocks, the PFS and PDEHPV blocks would appear to be well separated by the intervening P2VP block. In the selective solvent 2-propanol, the exact location of the PDEHPV blocks is more difficult to infer. Because of the limited solubility of PDEHPV in 2-propanol, we imagine that if the PDEHPV blocks were located exclusively at the periphery of the P2VP corona, there would be a strong tendency for the aggregation of the micelles through microphase separation of these blocks. While there is some micelle aggregation, as seen in Figure 2 and in Figure 7, there is little indication of aggregation in sonicated micelles, which are shorter in length. On this basis, we believe that many of the PDEHPV chains are buried within the P2VP corona of the micelles. This may be the environment responsible for the decrease of fluorescence quantum yield of the PDEHPV block in the micellar solution.

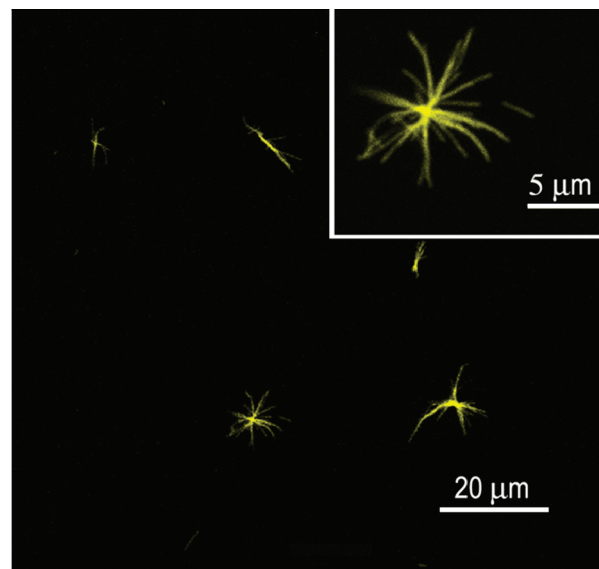


Figure 7. Laser confocal fluorescence microscopy images of PFS₃₀-*b*-P2VP₃₀₀-*b*-PDEHPV₁₃ micelles in the 2-propanol solution. The inset is at higher magnification.

The fluorescence of the PDEHPV chains in micelles suggests that laser confocal fluorescence microscopy (LCFM) might be useful for probing the structure of these species in solution. Several other groups have been able to image block copolymer micelles with μm dimensions by optical microscopy, especially by fluorescence microscopy.^{58–60} Solutions of the micelles were prepared as described above by heating samples of PFS₃₀-*b*-P2VP₃₀₀-*b*-PDEHPV₁₃ triblock copolymer in 2-propanol at 80 °C for 1 h, and diluting to 0.001 mg/mL after the solution cooled to room temperature. The images in Figure 7 are taken from a sample of the solution placed on a microscope slide and covered with a coverslip. The strong fluorescence from several micelles can be seen including one rod-like object in the upper center that appears to consist of two or more individual micelles. The similarity in shape of the flower-like micelle aggregate in the inset in Figure 7 to those seen in the TEM image in Figure 2A confirms that these shapes exist in solution and are not formed as the solution dries on the TEM grid. Sonicated micelles also fluoresce, but they are too small to be resolved clearly by LCFM.

Summary

We have demonstrated the synthesis of a new class of ferrocene-based amphiphilic polyferrocenylsilane triblock copolymers containing a π -conjugated poly(phenylvinylene) block. In this polymer, PFS₃₀-*b*-P2VP₃₀₀-*b*-PDEHPV₁₃, the PDEHPV block is separated from the PFS block by a long P2VP sequence. As a consequence, there is little quenching of the fluorescence of the PDEHPV block by the PFS block when the polymer is dissolved in a common good solvent such as THF. These polymers assemble into cylindrical micelles in 2-propanol, a poor solvent for PFS, a good solvent for P2VP, and a marginal solvent for PDEHPV. The limiting solubility of PDEHPV₁₃-CHO was determined to be 0.02 mg/mL in 2-PrOH. Long micelles (μm length) undergo secondary aggregation to form flower-like structures. There is no indication of aggregation when the micelles are shortened (< 300 nm) by sonication.

The PDEHPV-CHO block remains fluorescent in the micelles with a fluorescence quantum yield about 0.17. This allows one to image the micelle aggregates in solution by laser confocal fluorescence microscopy. These measurements establish that the flower-like micelle aggregates seen by TEM are also present in solution.

Acknowledgment. The authors thank NSERC Canada for their support of this research. GDS acknowledges the support of an EWR Steacie Memorial Fellowship. I.M. thanks the European Union for the Marie Curie Chair and the Royal Society for a Wolfson Research Merit Award. T.G. is grateful to the DFG for a postdoctoral fellowship. The authors also thank Dr. Hai Wang (Toronto) and Ms. Jessica Gwyther (Bristol) for helpful advice about the polymer synthesis.

Supporting Information Available: Figures showing GPC curves of PFS homopolymer by triple detection, the UV-vis spectra of PDEHPV₁₃-CHO in THF and 2-PrOH, plots of the maximum absorbances of PDEHPV₁₃-CHO as a function of their weight concentrations in THF, FT-IR spectra of PDEHPV₁₃-CHO and triblock copolymer, ¹H NMR spectrum of PDEHPV-CHO, PFS₃₀-*b*-P2VP₃₀₀, and PFS₃₀-*b*-P2VP₃₀₀-*b*-PDEHPV₁₃ triblock copolymer, and TEM images of diblock copolymer PFS₃₀-*b*-P2VP₃₀₀ micelles prepared in 2-propanol at 80 °C. This material is available free of charge via the Internet at <http://pubs.acs.org>.

References and Notes

- Archer, R. D. *Inorganic and Organometallic Polymers*; John Wiley & Sons: New York, 2001.
- Newkome, G. R.; He, E.; Moorefield, C. N. *Chem. Rev.* **1999**, *99*, 1689–1746.
- Astruc, D.; Chardac, F. *Chem. Rev.* **2001**, *101*, 2991–3023.
- Abd-El-Aziz, A. S.; Todd, E. K. *Coord. Chem. Rev.* **2003**, *246*, 3–52.
- Manners, I. *Science* **2001**, *294*, 1664–1666.
- Whittell, G. R.; Manners, I. *Adv. Mater.* **2007**, *19*, 3439–3468.
- Togni, A.; Hayashi, T. *Ferrocenes*; VCH Publishers: New York, 1995.
- Stanton, C. E.; Lee, T. R.; Grubbs, R. H.; Lewis, N. S.; Pudelski, J. K.; Callstrom, M. R.; Erickson, M. S.; McLaughlin, M. L. *Macromolecules* **1995**, *28*, 8713–8721.
- Eitouni, H. B.; Balsara, N. P. *J. Am. Chem. Soc.* **2004**, *126*, 7446–7447.
- Wang, X. S.; Wang, H.; Coombs, N.; Winnik, M. A.; Manners, I. *J. Am. Chem. Soc.* **2005**, *127*, 8924–8925.
- Wang, H.; Wang, X. S.; Winnik, M. A.; Manners, I. *J. Am. Chem. Soc.* **2008**, *130*, 12921–12930.
- Foucher, D. A.; Tang, B. Z.; Manners, I. *J. Am. Chem. Soc.* **1992**, *114*, 6246–6248.
- Roerdink, M.; van Zanten, T. S.; Hempenius, M. A.; Zhong, Z.; Feijen, J.; Vancso, G. J. *Macromol. Rapid Commun.* **2007**, *28*, 2125–2130.
- Lammertink, R. G. H.; Hempenius, M. A.; Thomas, E. L.; Vancso, G. J. *J. Polym. Sci., Part B: Polym. Phys.* **1999**, *37*, 1009–1021.
- Rider, D. A.; Cavicchi, K. A.; Power-Billard, K. N.; Russell, T. P.; Manners, I. *Macromolecules* **2005**, *38*, 6931–6938.
- Cheng, J. Y.; Ross, C. A.; Chan, V. Z. H.; Thomas, E. L.; Lammertink, R. G. H.; Vancso, G. J. *Adv. Mater.* **2001**, *13*, 1174–1178.
- Massey, J.; Power, K. N.; Manners, I.; Winnik, M. A. *J. Am. Chem. Soc.* **1998**, *120*, 9533–9540.
- Zhulina, E. B.; Adam, M.; LaRue, I.; Sheiko, S. S.; Rubinstein, M. *Macromolecules* **2005**, *38*, 5330–5351.
- Gädt, T.; Jeong, N. S.; Cambridge, G.; Winnik, M. A.; Manners, I. *Nat. Mater.* **2009**, *8*, 144–150.
- Lazzari, M.; Scalarone, D.; Hoppe, C. E.; Vazquez-Vazquez, C.; Lopez-Quintela, M. A. *Chem. Mater.* **2007**, *19*, 5818–5820.
- Lazzari, M.; Scalarone, D.; Vazquez-Vazquez, C.; Lopez-Quintela, M. A. *Macromol. Rapid Commun.* **2008**, *29*, 352–357.
- Du, Z. X.; Xu, J. T.; Fan, Z. Q. *Macromolecules* **2007**, *40*, 7633–7637.
- Portinha, D.; Boue, F.; Bouteiller, L.; Carrot, G.; Chassenieux, C.; Pensec, S.; Reiter, G. *Macromolecules* **2007**, *40*, 4037–4042.
- Schmalz, H.; Schmelz, J.; Drechsler, M.; Yuan, J.; Walther, A.; Schweimer, K.; Mihut, A. M. *Macromolecules* **2008**, *41*, 3235–3242.
- Lin, E. K.; Gast, A. P. *Macromolecules* **1996**, *29*, 4432–4441.
- Richter, D.; Schneiders, D.; Monkenbusch, M.; Willner, L.; Fetters, L. J.; Huang, J. S.; Lin, M.; Mortensen, K.; Farago, B. *Macromolecules* **1997**, *30*, 1053–1068.
- Cao, L.; Manners, I.; Winnik, M. A. *Macromolecules* **2002**, *35*, 8258–8260.
- Wang, X. S.; Winnik, M. A.; Manners, I. *Macromolecules* **2005**, *38*, 1928–1935.
- Massey, J. A.; Temple, K.; Cao, L.; Rharbi, Y.; Ræz, J.; Winnik, M. A.; Manners, I. *J. Am. Chem. Soc.* **2000**, *122*, 11577–11584.
- Wang, X. S.; Guerin, G.; Wang, H.; Wang, Y. S.; Manners, I.; Winnik, M. A. *Science* **2007**, *317*, 644–647.
- Guerin, G.; Wang, H.; Manners, I.; Winnik, M. A. *J. Am. Chem. Soc.* **2008**, *130*, 14763–14771.
- Corriu, R. J. P.; Devylder, N.; Guerin, C.; Henner, B.; Jean, A. *Organometallics* **1994**, *13*, 3194–3202.
- Yamamoto, T.; Morikita, T.; Maruyama, T.; Kubota, K.; Katada, M. *Macromolecules* **1997**, *30*, 5390–5396.
- Knapp, R.; Velten, U.; Rehahn, M. *Polymer* **1998**, *39*, 5827–5838.
- Buretea, M. A.; Tilley, T. D. *Organometallics* **1997**, *16*, 1507–1510.
- Heo, R. W.; Somoza, F. B.; Lee, T. R. *J. Am. Chem. Soc.* **1998**, *120*, 1621–1622.
- Masson, G.; Lough, A. J.; Manners, I. *Macromolecules* **2008**, *41*, 539–547.
- Janowska, I.; Zakrzewski, J.; Nakatani, K.; Palusiak, M.; Walak, M.; Scholl, H. *J. Organomet. Chem.* **2006**, *691*, 323–330.
- Tan, L.; Curtis, M. D.; Francis, A. H. *Macromolecules* **2002**, *35*, 4628–4635.
- Kanato, H.; Takimiya, K.; Otsubo, T.; Aso, Y.; Nakamura, T.; Araki, Y.; Ito, O. *J. Org. Chem.* **2004**, *69*, 7183–7189.
- Figueira-Duarte, T. M.; Rio, Y.; Listorti, A.; Delavaux-Nicot, W.; Holler, M.; Marchioni, F.; Ceroni, P.; Armaroli, N.; Nierengarten, J. F. *New J. Chem.* **2008**, *32*, 54–64.
- Morisaki, Y.; Murakami, T.; Chujo, Y. *J. Inorg. Organomet. Polym. Mater.* **2009**, *19*, 104–112.
- Chance, B.; Nishimura, M. *Proc. Natl. Acad. Sci. U.S.A.* **1960**, *46*, 19–24.
- Guldi, D. M.; Maggini, M.; Scorrano, G.; Prato, M. *J. Am. Chem. Soc.* **1997**, *119*, 974–980.
- Lakowicz, J. R. *Principles of Fluorescence Spectroscopy*, 2nd ed.; Kluwer Academic/Plenum: New York, 1999.
- Wang, H.; Winnik, M. A.; Manners, I. *Macromolecules* **2007**, *40*, 3784–3789.
- Ni, Y. Z.; Rulkens, R.; Manners, I. *J. Am. Chem. Soc.* **1996**, *118*, 4102–4114.
- Kretzschmann, H.; Meier, H. *Tetrahedron Lett.* **1991**, *32*, 5059–5062.
- Olsen, B. D.; Segalman, R. A. *Macromolecules* **2005**, *38*, 10127–10137.
- O'Connor, D. V.; Phillips, D. *Time Correlated Single Photon Counting*; Academic Press: London, 1984.
- Kloninger, C.; Knecht, D.; Rehahn, M. *Polymer* **2004**, *45*, 8323–8332.
- Kloninger, C.; Rehahn, M. *Macromolecules* **2004**, *37*, 1720–1727.
- Brandrup, J.; Immergut, E. H.; Grulke, E. A.; Grulke, E. A.; Bloch, D. *Polymer Handbook*, 4th ed.; John Wiley & Sons, Inc.: New York, 1999.
- Sary, N.; Rubatat, L.; Brochon, C.; Hadzioannou, G.; Ruokolainen, J.; Mezzenga, R. *Macromolecules* **2007**, *40*, 6990–6997.
- Resendes, R.; Massey, J. A.; Temple, K.; Cao, L.; Power-Billard, K. N.; Winnik, M. A.; Manners, I. *Chem.—Eur. J.* **2001**, *7*, 2414–2424.
- Shen, L.; Wang, H.; Guerin, G.; Wu, C.; Manners, I.; Winnik, M. A. *Macromolecules* **2008**, *41*, 4380–4389.
- Yang, J.; Cyr, P. W.; Wang, Y. S.; Soong, R.; Macdonald, P. M.; Chen, L. S.; Manners, I.; Winnik, M. A. *Photochem. Photobiol.* **2006**, *82*, 262–267.
- Jenekhe, S. A.; Chen, X. L. *Science* **1999**, *283*, 372–375.
- Wu, J.; Pearce, E. M.; Kwei, T. K. *Macromolecules* **2001**, *34*, 1828–1836.
- Dalhaimer, P.; Bates, F. S.; Discher, D. E. *Macromolecules* **2003**, *36*, 6873–6877.